The American Journal of Human Genetics

Supplemental Data

Mouse and Human *CRKL* Is Dosage Sensitive for Cardiac Outflow Tract Formation

Silvia E. Racedo, Donna M. McDonald-McGinn, Jonathan H. Chung, Elizabeth Goldmuntz, Elaine Zackai, Beverly S. Emanuel, Bin Zhou, Birgit Funke, and Bernice E. Morrow

Figure S1

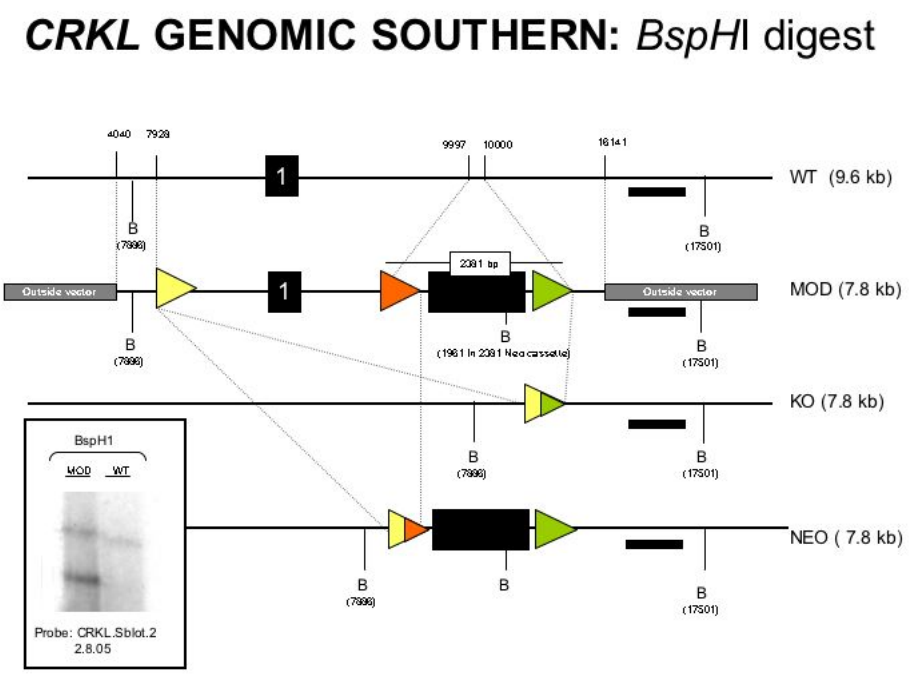
CRKL GENOMIC SOUTHERN: BspHI digest
4040
7928
9997
10000
16141
1
WT (9.6 kb)
B
(7898)
B
(17501)
2381 bp
Outside vector
MOD (7.8 kb)
(1961 in 2381 Neo cassette)
KO (7.8 kb)
BspH1
MOD
WT
NEO (7.8 kb)
Probe: CRKL.Sblot.2
2.8.05

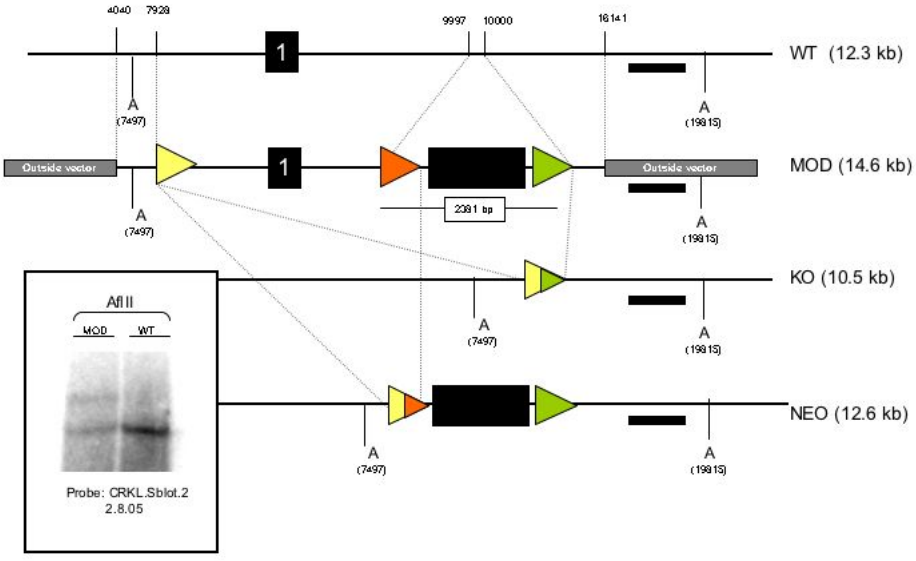
CRKL GENOMIC SOUTHERN: AflII digest
4040
7928
9997
10000
16141
1
WT (12.3 kb)
A
(7497)
A
(19815)
Outside vector
MOD (14.6 kb)
2381 bp
KO (10.5 kb)
AflII
MOD
WT
NEO (12.6 kb)
Probe: CRKL.Sblot.2
2.8.05

Figure S1. *Crkl* gene targeting to generate various alleles.
The mouse *Crkl* locus indicating the position of exon 1 is shown. The three-loxP sites are indicated as three different colors (yellow, orange and green triangles). The loxP sites flank exon 1 and either side of the Neomycin cassette (black box). The targeting construct and vector (gray boxes) are shown (MOD, 7.8 kb). Genomic Southern hybridization was performed to detect the correctly targeted *Crkl* allele. Two different digests of tail DNA was performed, one using *BspH*1 (left) and the other *Afl*II (right). A probe (black bar) was used outside the targeting construct, such that correct targeting could be detected. Bands of the correct targeted size were detected by genomic Southern blot hybridization.

Figure S2

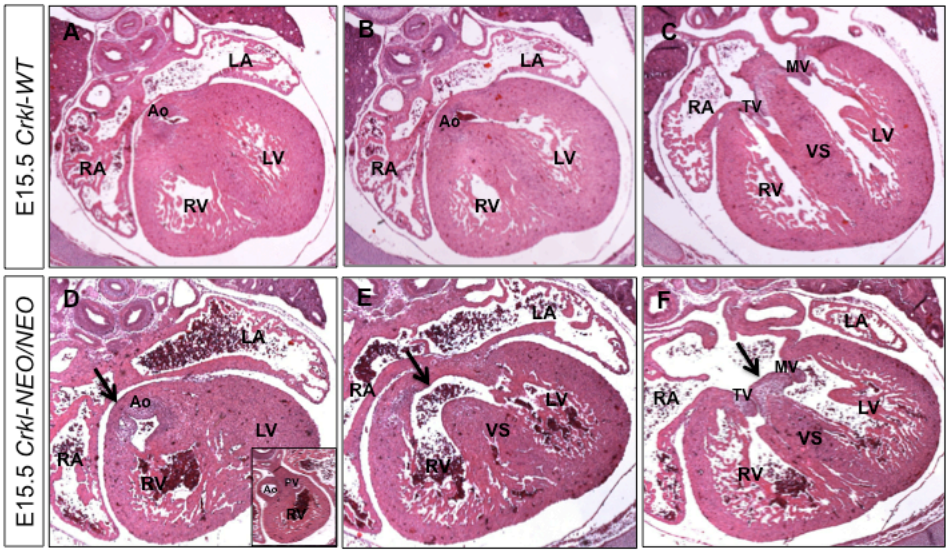

Figure S2. Overriding aorta and ventricular septal defect in a *Crkl-NEO/NEO* embryo.

Transverse histological sections of a *Crkl-WT* (A, B and C) versus *Crkl-NEO/NEO* embryonic mouse heart (D, E and F) at E15.5 stained with hematoxylin and eosin. Arrow (D) shows the aorta on top of RV (Ao). Inset (D) shows the aortic valve and the pulmonary valve at the same level. Arrow (E) shows a VSD and (F) denotes atrioventricular cushions with blunted valves. RA = right atrium, RV = right ventricle, LA = left atrium, LV= left ventricle, Ao = Aorta, PV = pulmonary valve, VS = ventricular septum.

Figure S3

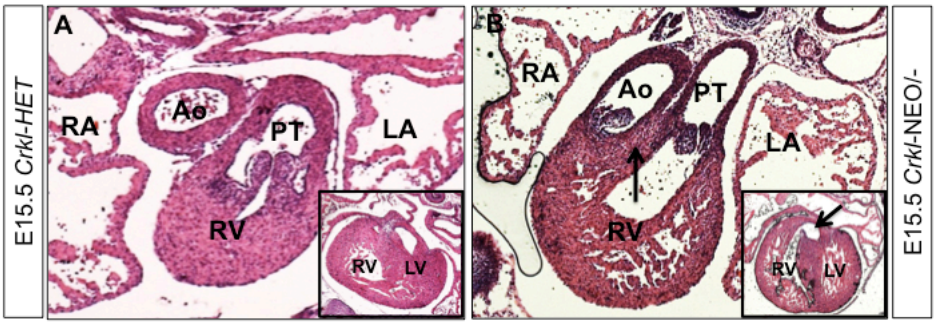

Figure S3. Double outlet right ventricle in a *Crkl-NEO/-* embryo.
Transverse histological sections of the aorta and pulmonary trunk or heart (inset) in a *Crkl-HET* (A) versus *Crkl-NEO/-* embryo (B) at E15.5 stained with hematoxylin and eosin. Normally, the aorta and pulmonary trunk do not enter the right ventricle (A). Arrow (B) shows the aorta and the pulmonary trunk connected to the RV in the *Crkl-NEO/-* embryo. In the *Crkl-NEO/-* embryo, a VSD is also present (arrow in inset in B), which is absent in the heterozygous embryo (inset in A). RA = right atrium, RV = right ventricle, LA = left atrium, LV= left ventricle, Ao = Aorta, PT = pulmonary trunk.

Table S1

PATIENT ID#	DELETION TYPE	Cardiac diagnosis of new cohort of patients (probands)
11701-A	B-D	Normal echo
11702-A	B-D	Normal echo
11707-A	B-D	Normal echo and MRI
11745-A	B-D	Normal Echo
11762	B-D	TOF
11772-A	B-D	VSD/ASD
11773-A	B-D	PTA
11782-A	B-D	Normal echo
11783-A	B-D	IAAB/VSD/bicuspid aortic valve
11784-A	B-D	TOF
11812-A	B-D	Normal echo
11952-A	B-D	Normal echo
12001	B-D	Normal echo
12039-A	B-D	VSD/ASD
12040-A	B-D	Normal echo
12085-A	B-D	Normal echo
12086	B-D	Normal echo
12098-A	B-D	VSD/bicuspid aortic valve/severe discrete coarcation of the aorta
12145	B-D	VSD
12167	B-D	Normal echo
11687	C-D	Normal echo
11916	C-D	Normal echo
12144	C-D	TOF
12150	C-D	Normal echo
12164	C-D	Normal echo

Table S1. List of patients ascertained.
Twenty new LCR22B-D (B-D) and five LCR22C-D (C-D) probands are shown with their identification numbers and cardiac diagnoses. Echo is an abbreviation for echocardiogram. TOF, VSD, ASD, IAAB = interrupted aortic arch type B, PTA.

Table S2

ALLELIC COMBINATION			*Crkl-WT*	*Crkl-NEO/+*	*Crkl-HET*	*Crkl-NEO/NEO*	*Crkl-NEO/-*	*Crkl-KO*
CARDIAC PHENOTYPE E15.5			n/N (%)	n/N (%)	n/N (%)	n/N (%)	n/N (%)	n/N (%)
OFT ALIGNMENT	OVERRIDING Ao (OA)		-	-	-	5/25 (20)	-	-
	DORV		-	-	-	2/25 (8)	10/15 (67)	5/24 (21)
	TOF		-	-	-	1/25 (4)	3/15 (20)	6/24 (25)
VENTRICLES	VSD		-	-	-	9/25 (36)	13/15 (87)	11/24 (46)
	THICKNESS	Thick RV	-	-	-	1/25 (4)	3/15 (20)	6/24 (25)
		Thin RV	-	-	-	2/25 (8)	10/15 (67)	5/24 (21)
ASD			-	-	-	1/25 (4)	-	1/24 (4)
NO DEFECTS			23/23 (100)	20/20 (100)	11/11 (100)	4/25 (16)	2/15 (13)	0/24 (0)

Table S2. Cardiac phenotypes in embryonic hearts from the *Crkl* allelic series.
The different genotypes that were generated from the different *Crkl* alleles are listed in the first row of the Table. OFT alignment defects are listed as one category. DORV; TOF. Various intracardiac defects included VSD and defects in the thickness of the myocardium, including thicker (hypertrophic) or thinner (dilated) muscular wall of the right ventricle in association with other defects. Few embryos had ASDs. Note that approximately 15% of *Crkl-NEO/NEO* or *Crkl-NEO/-* embryos had no detectable heart defects. The severity and types of defects vary among the different alleles.

Table S3

Gene symbol	HUGO gene name	Strand	cdsStart	cdsEnd	Exon Count	LCR22	Function	PMID
ZNF74	Zinc finger protein 74	+	20748918	20759946	4	B-C	May function in RNA maturation and transcriptional regulation; present in the nuclear matrix	1 2 ,
SCARF2	Scavenger receptor class F, member 2	-	20779664	20792041	12	B-C	Recessive mutations cause Van Den Ende-Gupta syndrome; craniofacial features, skeletal abnormalities. Ca+ binding protein in epidermis.	3 4 ,
KLHL22	Kelch-like family member 22	-	20796359	20843498	7	B-C	Adaptor protein that works with other proteins to regulate chromosome alignment during mitosis.	5 6 ,
MED15	Mediator complex subunit 15	+	20861965	20940991	18	B-C	Transcrptional coactivator in RNA polymerase II transcription; Part of Mediator complex.	7 8 ,
PI4KA	Phosphatidylinositol 4-kinase, catalytic, alpha	-	21062334	21213013	55	C-D	Catalyzes first step in biosynthesis of phosphatidylinositol 4,5-bisphosphate; knockout mice show early embryonic lethality.	9 10 ,
SERPIND1	Serpin peptidase inhibitor, clade D; also called Heparin cofactor II	+	21133600	21141354	5	C-D	Serine proteinase inhibitor that inhibits thrombin in coagulation cascade; Regulates angiogenesis	11 12 , 13 ,
SNAP29	Synaptosomal-associated protein, 29kDa	+	21213398	21242124	5	C-D	Synaptic vesicle membrane docking; gene for Cednik syndrome (cerebral dysgenesis, neuropathy, ichthyosis, keratoderma)	14 15 ,

CRKL	v-crk avian sarcoma virus CT10 oncogene homolog-like	+	21272222	21304133	3	C-D	Cytoplasmic adaptor to receptor tyrosine kinases; MAPK pathway	16 17 ,
LOC101928891		+	21318968	21318968	2	C-D		
AIFM3	Apoptosis-inducing factor, mitochondrion-associated, 3; alias, AIFL	+	21322232	21335320	21	C-D	Target gene of miR-210, induced by hypoxia.	18
LZTR1	Leucine-zipper-like transcription regulator 1	+	21336660	21351637	21	C-D	BTB-kelch superfamily gene, localizes to the Golgi network. Mutations (autosomal dominant with SMARCB1 mutations) cause multiple schwannomas.	19 20 ,
THAP7	THAP domain containing 7	-	21354168	21356200	5	C-D	Chromatin modifier; targets deacetylation of histone; recruits HDAC3	21 22 ,
P2RX6	Purinergic receptor P2X, ligand-gated ion channel, 6	+	21369463	21380906	12	C-D	P2X receptors, ATP-gated ion channels in skeletal muscle. Associated with cadherin in endothelial cells.	23 24 ,
SLC7A4	Solute carrier family 7, member 4	-	21383343	21386101	5	C-D	Similar to cationic amino acid transporters	25
LRRC74B	Leucine rich repeat containing 74B	+	21400275	21414817	10	C-D		

Table S3. The genes in the LCR22B-D interval.
The gene symbol, detailed coordinates, full name, exon number, location (B-C; C-D), biological functional information from the literature are indicated.

1. Grondin, B., Cote, F., Bazinet, M., Vincent, M., and Aubry, M. (1997). Direct interaction of the KRAB/Cys2-His2 zinc finger protein ZNF74 with a hyperphosphorylated form of the RNA polymerase II largest subunit. The Journal of biological chemistry 272, 27877-27885.
2. Cote, F., Boisvert, F.M., Grondin, B., Bazinet, M., Goodyer, C.G., Bazett-Jones, D.P., and Aubry, M. (2001). Alternative promoter usage and splicing of ZNF74 multifinger gene produce

protein isoforms with a different repressor activity and nuclear partitioning. DNA and cell biology 20, 159-173.
3. Hwang, J., Kalinin, A., Hwang, M., Anderson, D.E., Kim, M.J., Stojadinovic, O., Tomic-Canic, M., Lee, S.H., and Morasso, M.I. (2007). Role of Scarf and its binding target proteins in epidermal calcium homeostasis. The Journal of biological chemistry 282, 18645-18653.
4. Anastasio, N., Ben-Omran, T., Teebi, A., Ha, K.C., Lalonde, E., Ali, R., Almureikhi, M., Der Kaloustian, V.M., Liu, J., Rosenblatt, D.S., et al. (2010). Mutations in SCARF2 are responsible for Van Den Ende-Gupta syndrome. American journal of human genetics 87, 553-559.
5. Maerki, S., Olma, M.H., Staubli, T., Steigemann, P., Gerlich, D.W., Quadroni, M., Sumara, I., and Peter, M. (2009). The Cul3-KLHL21 E3 ubiquitin ligase targets aurora B to midzone microtubules in anaphase and is required for cytokinesis. The Journal of cell biology 187, 791-800.
6. Beck, J., Maerki, S., Posch, M., Metzger, T., Persaud, A., Scheel, H., Hofmann, K., Rotin, D., Pedrioli, P., Swedlow, J.R., et al. (2013). Ubiquitylation-dependent localization of PLK1 in mitosis. Nature cell biology 15, 430-439.
7. Conaway, R.C., and Conaway, J.W. (2011). Origins and activity of the Mediator complex. Seminars in cell & developmental biology 22, 729-734.
8. Kim, S., and Gross, D.S. (2013). Mediator recruitment to heat shock genes requires dual Hsf1 activation domains and mediator tail subunits Med15 and Med16. The Journal of biological chemistry 288, 12197-12213.
9. Vaillancourt, F.H., Brault, M., Pilote, L., Uyttersprot, N., Gaillard, E.T., Stoltz, J.H., Knight, B.L., Pantages, L., McFarland, M., Breitfelder, S., et al. (2012). Evaluation of phosphatidylinositol-4-kinase IIIalpha as a hepatitis C virus drug target. Journal of virology 86, 11595-11607.
10. Bojjireddy, N., Botyanszki, J., Hammond, G., Creech, D., Peterson, R., Kemp, D.C., Snead, M., Brown, R., Morrison, A., Wilson, S., et al. (2014). Pharmacological and genetic targeting of the PI4KA enzyme reveals its important role in maintaining plasma membrane phosphatidylinositol 4-phosphate and phosphatidylinositol 4,5-bisphosphate levels. The Journal of biological chemistry 289, 6120-6132.
11. Aihara, K., Azuma, H., Akaike, M., Sata, M., and Matsumoto, T. (2009). Heparin cofactor II as a novel vascular protective factor against atherosclerosis. Journal of atherosclerosis and thrombosis 16, 523-531.
12. Ikeda, Y., Aihara, K., Yoshida, S., Iwase, T., Tajima, S., Izawa-Ishizawa, Y., Kihira, Y., Ishizawa, K., Tomita, S., Tsuchiya, K., et al. (2012). Heparin cofactor II, a serine protease inhibitor, promotes angiogenesis via activation of the AMP-activated protein kinase-endothelial nitric-oxide synthase signaling pathway. The Journal of biological chemistry 287, 34256-34263.
13. Kumar, A., Bhandari, A., Sarde, S.J., and Goswami, C. (2014). Genetic variants and evolutionary analyses of heparin cofactor II. Immunobiology 219, 713-728.
14. Fuchs-Telem, D., Stewart, H., Rapaport, D., Nousbeck, J., Gat, A., Gini, M., Lugassy, Y., Emmert, S., Eckl, K., Hennies, H.C., et al. (2011). CEDNIK syndrome results from loss-of-function mutations in SNAP29. The British journal of dermatology 164, 610-616.
15. McDonald-McGinn, D.M., Fahiminiya, S., Revil, T., Nowakowska, B.A., Suhl, J., Bailey, A., Mlynarski, E., Lynch, D.R., Yan, A.C., Bilaniuk, L.T., et al. (2013). Hemizygous mutations in SNAP29 unmask autosomal recessive conditions and contribute to atypical findings in patients with 22q11.2DS. Journal of medical genetics 50, 80-90.
16. Guris, D.L., Fantes, J., Tara, D., Druker, B.J., and Imamoto, A. (2001). Mice lacking the homologue of the human 22q11.2 gene CRKL phenocopy neurocristopathies of DiGeorge syndrome. Nature genetics 27, 293-298.
17. Moon, A.M., Guris, D.L., Seo, J.H., Li, L., Hammond, J., Talbot, A., and Imamoto, A. (2006). Crkl deficiency disrupts Fgf8 signaling in a mouse model of 22q11 deletion syndromes. Developmental cell 10, 71-80.

18. Yang, W., Sun, T., Cao, J., Liu, F., Tian, Y., and Zhu, W. (2012). Downregulation of miR-210 expression inhibits proliferation, induces apoptosis and enhances radiosensitivity in hypoxic human hepatoma cells in vitro. Experimental cell research 318, 944-954.
19. Nacak, T.G., Leptien, K., Fellner, D., Augustin, H.G., and Kroll, J. (2006). The BTB-kelch protein LZTR-1 is a novel Golgi protein that is degraded upon induction of apoptosis. The Journal of biological chemistry 281, 5065-5071.
20. Piotrowski, A., Xie, J., Liu, Y.F., Poplawski, A.B., Gomes, A.R., Madanecki, P., Fu, C., Crowley, M.R., Crossman, D.K., Armstrong, L., et al. (2014). Germline loss-of-function mutations in LZTR1 predispose to an inherited disorder of multiple schwannomas. Nature genetics 46, 182-187.
21. Macfarlan, T., Kutney, S., Altman, B., Montross, R., Yu, J., and Chakravarti, D. (2005). Human THAP7 is a chromatin-associated, histone tail-binding protein that represses transcription via recruitment of HDAC3 and nuclear hormone receptor corepressor. The Journal of biological chemistry 280, 7346-7358.
22. Macfarlan, T., Parker, J.B., Nagata, K., and Chakravarti, D. (2006). Thanatos-associated protein 7 associates with template activating factor-Ibeta and inhibits histone acetylation to repress transcription. Molecular endocrinology 20, 335-347.
23. Yu, Q., Zhao, Z., Sun, J., Guo, W., Fu, J., Burnstock, G., He, C., and Xiang, Z. (2010). Expression of P2X6 receptors in the enteric nervous system of the rat gastrointestinal tract. Histochemistry and cell biology 133, 177-188.
24. Hausmann, R., Bodnar, M., Woltersdorf, R., Wang, H., Fuchs, M., Messemer, N., Qin, Y., Gunther, J., Riedel, T., Grohmann, M., et al. (2012). ATP binding site mutagenesis reveals different subunit stoichiometry of functional P2X2/3 and P2X2/6 receptors. The Journal of biological chemistry 287, 13930-13943.
25. Wolf, S., Janzen, A., Vekony, N., Martine, U., Strand, D., and Closs, E.I. (2002). Expression of solute carrier 7A4 (SLC7A4) in the plasma membrane is not sufficient to mediate amino acid transport activity. The Biochemical journal 364, 767-775.